

Thermal Evaluation of Material Extrusion Process Parameters and Their Impact on Warping Deformation

Hussein Alzyod*, Peter Ficzer

Department of Railway Vehicles and Vehicle System Analysis, Faculty of Transportation Engineering and Vehicle Engineering, Budapest University of Technology and Economics, H-1111 Budapest Műegyetem rkp. 3.

Received 12 Jul 2023

Accepted 30 Aug 2023

Abstract

Warping deformation poses a significant challenge in the material extrusion process of ABS additive manufacturing, impacting dimensional accuracy and part quality. In this study, we aimed to optimize the printing factors to minimize warping deformation and enhance the overall performance of ABS-printed parts. The studied parameters included bed temperature, printing speed, chamber temperature, and printing temperature. To overcome the limitations of time-consuming and costly laboratory experiments, a simulation-based approach using numerical techniques and the Digimat-AM software's finite element model was employed to visualize and analyze warping deformation. The Taguchi technique was utilized to design a series of experiments, yielding valuable data for statistical analysis and optimization. The results highlighted the significant influence of bed temperature on warping deformation, followed by chamber temperature, printing temperature, and printing speed. Through systematic analysis, the "optimal" parameter settings were determined. These findings offer valuable insights for process optimization, enabling improved dimensional accuracy and reduced warping deformation in ABS additive manufacturing. By combining numerical simulation and the Taguchi method, this investigation gives a practical and efficient method for enhancing the performance of material extrusion processes, ensuring high-quality printed parts in the field of additive manufacturing.

© 2023 Jordan Journal of Mechanical and Industrial Engineering. All rights reserved

Keywords: Warping deformation, Material extrusion, Fused deposition modeling, Finite Element Analysis, Taguchi method, ANOVA.

1. Introduction

Additive manufacturing (AM), also known as a 3D printing technology, was invented by Charles Hull in the mid-80s of the last century[1]. Since then, AM technology has been developed rapidly and improved using many methods, but all of them use the same principle, layer upon layer. These days, it is employed in many industrial sectors, including aerospace[2], automotive [3], medical[4], [5], and even food[6]. AM manufacturing is categorized based on the raw material into four main categories, liquid, filament, powder, and solid layer[7]. In the filament category, Material Extrusion (MEX), also known as Fused Filament Fabrication (FFF) or Fused Deposition Modeling (FDM), which is trademarked to Stratasys since 1991 [8]. FFF is a low-cost and multilateral-using technology, making it one of users' most favored technologies. The use of polymer AM in the market in 2020 was estimated at about \$11 billion, and in 2030, it is expected to achieve more than \$55 billion[9]. As illustrated in **Figure 1**, MEX mainly has five components: filament, feeder, liquefier, nozzle, and bed plate.

The printing process begins by pulling the filament to the liquefier using the feeder. Two types of techniques are used in the feeding process, either Bowden or Direct[10]. Then, the liquefier melt the filament material to a semi-molten state prior to extrusion through the extruder head. Finally, the extruded

filament will be deposited on the bed plate and bond with the previous filament forming the layer. Building layers occurs with a fixed nozzle and moving bed plate or vice versa. MEX technology has structural and printing parameters, which can be identified in the slicing process, and **Figure 2** displays these parameters[11].

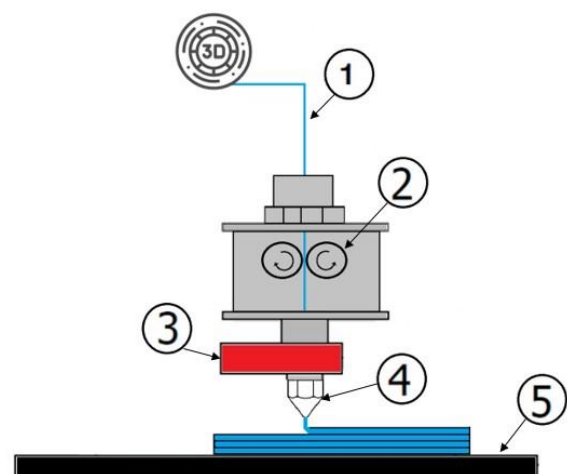


Figure 1. FFF schematic drawing: 1) filament, 2) feeder, 3) liquefier, 4) extruder head, and 5) bed plate

* Corresponding author e-mail: Hussein.alzyod@edu.bme.hu.

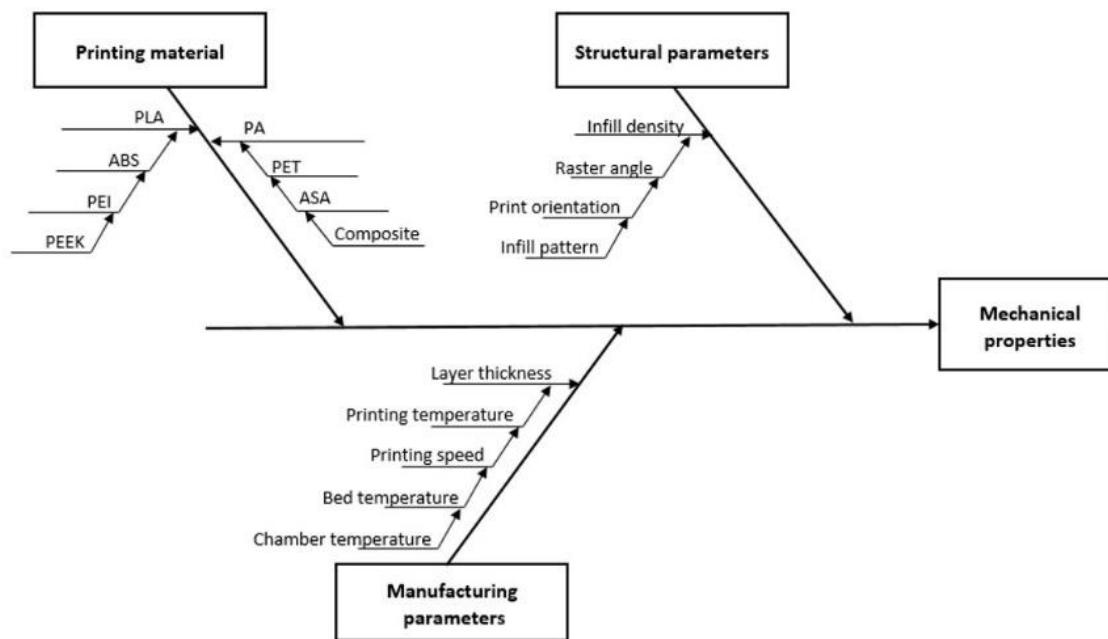


Figure 2. Ishikawa diagram of FFF parameters [11]

Most of commercial printers use open-source slicers, while industrial printers have their own slicers. The difference between open-source and non-open-source slicers is that the former can modify all the printing and structural parameters, while the latter has limitations regarding some parameters, such as extrusion temperature, extrusion speed, and infill pattern. MEX technology exhibits several promising benefits, encompassing its cost-effectiveness, versatility in material compatibility and biodegradable polymers [12], [13], ability to produce mechanically robust parts, compatible with reinforced and composite material, which hold significant importance by enabling the creation of lightweight yet strong components [14], [15], user-friendly operation, easy maintenance, and implementation, as well as its non-toxic nature [16]. Conversely, MEX does present certain limitations, including constraints on printing size, the requirement for support structures, extended build time, relatively low resolution, warping deformation, and limited accuracy. The extensive adoption of MEX technology has resulted in a surge of scientific research and inquiries [17]–[21]. Tura [22] studied the impact of four printing factors on the flexural strength of Acrylonitrile Butadiene Styrene (ABS) made using FFF technology, and he observed that the raster was the most important parameter. Hameed et al. [23] investigated five printing factors, and their impact on the tensile, flexural, and impact strength of Acrylonitrile Styrene Acrylate (ASA) fabricated using FDM technology. The research findings indicated that the infill density and layer height emerged as the primary factors influencing the results in the production of 3D-printed components. Beşliu-Băncescu et al. [24] examined the impact of printing temperature, layer thickness, and printing speed on the physical-mechanical properties (fracture temperature, weight error, ultimate tensile strength) as well as technological properties (cutting machinability, top and lateral surface roughness) of polycaprolactone (PCL) wood-based biopolymer components produced through FDM. The conducted research found that selecting the highest level of printing speed had a beneficial impact on both the surface roughness and ultimate tensile strength of the 3D-printed components. The machinability of these printed parts was assessed by analyzing cutting force criteria. The findings revealed that the PCL wood-based polymer, which was the

focus of this study, exhibited lower machinability compared to natural wood. Zhen et al. [25] conducted an impressive study to investigate the effect of filling angle, printing rate, printing orientation, and heat treatment effects on mechanical properties (tensile and bending) and crystallinity of Poly-ether-ether-ketone (PEEK) samples printed using FDM technology. The findings revealed that optimal mechanical performance was attained by employing a printing rate equivalent to one times the standard rate. Variation in angle cross-fillings within $\pm 10^\circ$ intervals, combined with vertical printing, also yielded favorable outcomes. It was observed that horizontal printing led to reduced warping. Moreover, heat treatment played a crucial role in enhancing both mechanical properties and crystallinity. Specifically, the most favorable outcomes were observed after subjecting the material to a heat treatment of 300°C for two hours. Notably, the measured tensile strength approached approximately 80% of the strength exhibited by injection-molded PEEK components. Previous research has been done to study the warping deformation in the MEX technology. Rosli et al. [26] studied the influence of bed temperature on the warping deformation of ABS-FDM parts and found that a decrease in warping was observed as the bed temperature increased. This outcome can be attributed to the reduction in thermal stress due to the higher glass transition temperature exhibited by the printed samples compared to the filament used. Chohan [27] utilized the Learning Enthusiasm based teaching-learning algorithm (LebTLBO) to optimize four printing factors and enhance the warping deformation of ABS components. In a separate study, Messimer et al. [28] examined the warping deformation of ten different materials by two types of heated plates: an aluminum-polycarbonate (AL-PC) composite and pure glass or aluminum plate. The findings indicated that utilizing a heated AL-PC print bed positively impacted the deformation of FDM samples, especially for TPU and ABS filaments. Chaidas [29] came to the conclusion that for Wood-flour PLA (PLA/W) composite material produced via FFF, lower printing temperature and layer thickness could optimize both surface quality and dimensional accuracy. Additionally, Vyavahare [30] identified wall print speed, layer thickness, and build orientation as important process parameters affecting the dimensional accuracy of ABS-FFF components.

Warping deformation, which significantly impacts dimensional accuracy and the quality of parts, occurs due to temperature variations between consecutive printed layers during the cooling and solidification process in 3D printing. It can also arise from temperature differences between the initial layer and the printer bed, leading to material shrinkage. The physical constraints exerted by the preceding layers give rise to warping deformation [31], and **Figure 3** depicts this phenomenon.

Consequently, the cooling behavior of layers plays a crucial role in the overall part quality and dimensional stability. After a new track is deposited, the layers beneath it undergo a cooling process due to the temperature gradient between the printing temperature and the surrounding environment[32]. This cooling process involves the transfer of heat through various mechanisms. The first mechanism is conductive heat transfer, where heat flows from the newly deposited track to the layers below it. Since these lower layers are already at a lower temperature, the heat transfer happens because of the temperature difference, causing the material to gradually cool and solidify[33]. This conductive heat transfer helps maintain the part's structural integrity as the layers solidify and bond together. The second mechanism is convective heat transfer, which involves heat exchange between the part and the surrounding air. The newly deposited track releases heat, creating a temperature gradient that promotes airflow around the part. This convective heat transfer allows for heat dissipation from the part to the ambient air, aiding in the cooling process[34]. Efficient convective heat transfer helps prevent overheating and ensures consistent cooling across the part. The third mechanism is radiative heat transfer, whereby heat is transferred through thermal radiation. The part, including the newly deposited track, emits thermal radiation that transfers heat to the rest of the part and the build chamber[35]. This radiative heat transfer contributes to the overall cooling of the part by dissipating heat energy in the form of electromagnetic radiation.

By considering these three heat transfer mechanisms, namely conductive, convective, and radiative, one can gain a comprehensive understanding of the thermal dynamics involved in the cooling process of FDM-printed parts. Optimizing these heat transfer processes is essential for controlling the cooling rate, minimizing warping, and achieving dimensional accuracy in the final printed parts. In light of the abovementioned heat transfer mechanisms in FDM printing, this research endeavors to shed light on the novel

investigation of the influence of four key printing factors, namely bed temperature, printing speed, chamber temperature, and printing temperature, on the warping deformation of ABS-FFF samples. The primary objective of this study is to employ numerical simulation techniques to comprehensively analyze the impact of these factors on warping deformation. Furthermore, to effectively explore the parameter space and ensure a robust experimental design, the Taguchi L9 orthogonal array methodology was utilized. Aligned with the investigation of these pivotal parameters, it is pertinent to acknowledge a prior empirical exploration of the same variables—bed temperature, printing speed, chamber temperature, and printing temperature. This antecedent experimental study laid the groundwork by providing tangible insights into the effects of these parameters on warpage deformation within the MEX process. Expanding upon this foundational work, our current research endeavors to complement and extend these empirical observations through the adoption of a numerical simulation approach, employing Finite Element Analysis (FEA), to rigorously scrutinize the same set of parameters. The incorporation of FEA within our study serves a dual purpose: it facilitates a comprehensive investigation into the intricate thermal dynamics and their resultant impact on warpage deformation, while concurrently offering a mechanism for validating the precision and dependability of our numerical methodology. By comparing our numerical outcomes with the empirical data generated by the preceding experimental study done by Stephens et al. [36], our objective is to establish a robust framework that substantiates the predictive capacity of our numerical solution in effectively elucidating the intricate interplay between process parameters and warpage deformation. This not only bolsters the authenticity of our findings but also contributes to the substantiation of numerical simulation as a potent avenue for comprehending the intricacies of the material extrusion process. Through the amalgamation of empirical insights and numerical validation, our research seeks to construct a holistic comprehension of how these parameters orchestrate warpage deformation within the realm of ABS additive manufacturing. This fusion of empirical knowledge and numerical rigor not only augments the existing academic corpus but also underscores the efficacy of a holistic approach in advancing the optimization of material extrusion procedures, thereby elevating part quality and dimensional precision to new thresholds.

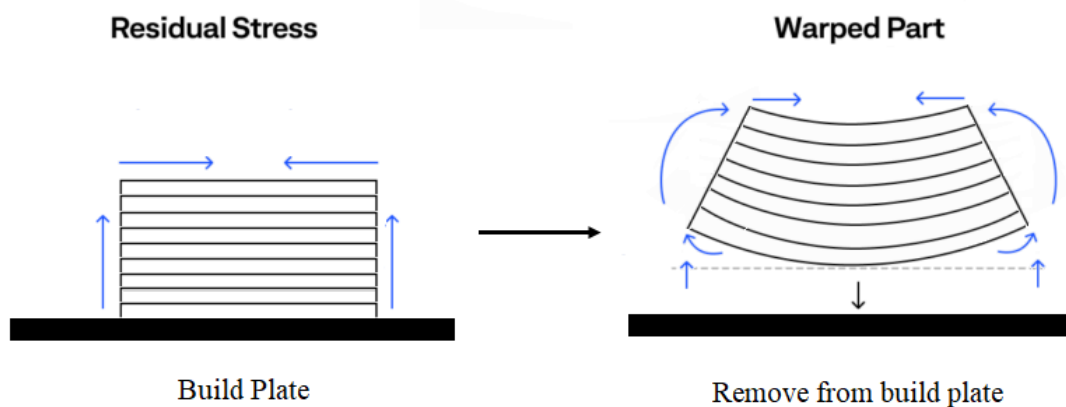


Figure 3. Development of warping deformation due to shrinkage and residual stress

2. Experiment details and methodology

2.1. Material, part, and printing factors

The ABS filament, utilized as a printing material in this investigation, was obtained from e-Xtream Engineering, which is a division of Hexagon's Manufacturing Intelligence. The filament used was a natural-colored, amorphous, and unfilled. A 3D cuboid model with specific dimensions of 60 mm x 30 mm x 10 mm was designed using computer-aided design (CAD) software to conduct the experiments. The design of the cuboid model is visually represented in **Figure 4**.

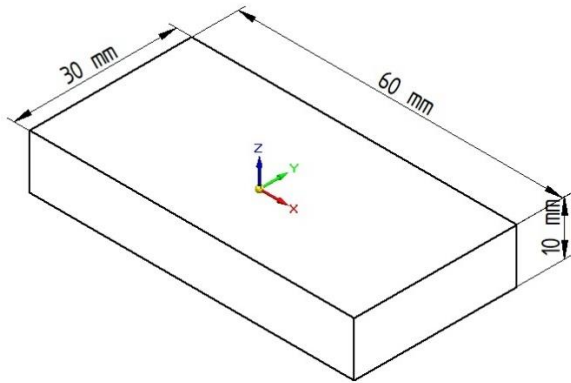


Figure 4. The sample used and its dimensions

2.2. Experimental design and optimizing method

To thoroughly investigate the influence of printing factors in MEX, it is essential to employ systematic design of experiments (DOE) approaches, such as Central Composite Design (CCD), Taguchi's method design, Box-Behnken design (BBD), and Response Surface Methodology (RSM) [37], [38]. These methods are pivotal in enabling a comprehensive analysis [39]. By adopting these DOE methods, researchers can systematically examine the impact of several input variables on a single output variable. This structured approach facilitates more precise representation of the response surface and aids in identifying optimum parameters setup [17]. Utilizing these DOE methods enhances the reliability and efficiency of the study, enabling researchers to draw meaningful conclusions about the effects of process factors in MEX. In this research, the Taguchi L9 orthogonal array methodology, useful in minimizing the number of experimental studies required to comprehensively analyze the various factors influencing performance parameters [40], was employed to analyze the four factors and their respective levels systematically. **Table 1** presents an overview of these factors and their designated levels for the experimental design. To assess and optimize the process variability and response values Mean Effects Plot (MEP) and Signal to Noise (S/N) ratio were utilized as analytical tools [41]. The selection of the S/N ratio type is contingent upon the study's specific objectives. In this investigation, the primary focus was on minimizing the warping deformation of the samples.

Table 1. Investigated factors and their levels

| Parameter | Unit | Levels | | |
|---------------------------|------|--------|-----|-----|
| | | 1 | 2 | 3 |
| Printing Temperature (PT) | °C | 225 | 230 | 235 |
| Bed Temperature (BT) | °C | 87 | 90 | 93 |
| Printing speed (PS) | mm/s | 30 | 45 | 60 |
| Chamber Temperature (CT) | °C | 37 | 40 | 43 |

Accordingly, the "smaller is better" type of S/N ratio was calculated according to Eq (1) as the appropriate criterion for evaluation [18], [42].

$$S/N = (-10) \times \log_{10} \left(\frac{1}{n} \sum_{i=1}^n y_i^2 \right) \quad (1)$$

These factors were selected due to their influence on the conductive, convective, and radiative heat transfer processes in MEX printing. The role of each parameter in relation to these heat transfer mechanisms can be illustrated as follows:

- **Printing Temperature:** The printing temperature primarily affects conductive heat transfer [43]. Higher printing temperatures lead to increased heat transfer from the newly deposited track to the layers below via conduction. It promotes better interlayer bonding by ensuring effective fusion and melting of the material. However, excessively high temperatures can result in excessive heat accumulation, leading to issues like over-melting and deformation.
- **Bed Temperature:** The bed temperature influences both conductive and convective heat transfer [44]. Maintaining an adequate bed temperature helps maintain the heat balance throughout the part. It aids in conducting heat to the layers below, ensuring proper interlayer adhesion and minimizing warping. Additionally, the bed temperature affects convective heat transfer by influencing the temperature gradient between the part and the surrounding air, facilitating heat dissipation from the part.
- **Chamber Temperature:** The chamber temperature predominantly impacts convective heat transfer [45]. Adjusting the chamber temperature allows to control the heat exchange between the part and the surrounding air. Higher chamber temperatures promote better convective cooling as the temperature gradient between the part and the air increases, facilitating more efficient heat dissipation. However, extreme temperature variations may also affect the dimensional stability of the part.
- **Printing Speed:** Printing speed affects all three heat transfer mechanisms to varying degrees [46]. Higher printing speeds can result in reduced heat transfer through conductive mechanisms, as the newly deposited material spends less time in contact with the previously printed layers. However, faster printing speeds can also impact convective heat transfer by altering the airflow patterns around the part. It may hinder effective cooling if the convective heat transfer is impeded. Additionally, printing speed can influence radiative heat transfer indirectly by affecting the overall heat accumulation within the part.

2.3. Numerical simulation

In recent years, the numerical solution has been implemented many sectors of research field [47]–[49]. AM technologies also utilized the numerical solution [50]. It saves time and money and can give a rapid prediction of the responses [51]. In this investigation, Digimat-AM FEA was employed to perform the simulation. Digimat-AM is a software tool that facilitates the simulation of additive manufacturing processes involving polymers and composites. Its primary purpose is to predict the warping and residual stress in 3D-MEX printed parts. The simulation procedure encompasses four main stages: definition, manufacturing, simulation, and results. Digimat-AM offers three manufacturing techniques during the definition stage: Selective Laser Sintering (SLS), FFF, and FDM. FFF was selected as the preferred technique for the specific task at hand. The FFF setup involved a chamber with dimensions of 200x200x180 mm, a fixed platform, and the application of a thermo-mechanical investigation method. The 3D printer settings in the slicer

software determined the dimensions of the chamber. In this stage, the geometry of the component was imported, while the chosen printing material was as mentioned before, ABS. Moving on to the manufacturing stage, the process steps were defined in a specific order: printing, holding, cooling, and removing support. This stage involved establishing the process factors. The room temperature was set at 25°C, while the chamber temperature was changed according to the investigated run, and a convection coefficient of 0.015 mW/mm² °C was applied. In the simulation stage, the user could choose between two options for geometry discretization: layer-by-layer discretization or filament discretization. The present study employed a layer-by-layer strategy within the filament discretization approach. Finite element layers were utilized instead of considering a section of the filament. The simulation was performed on a computer with an Intel(R) Core(TM) i7 CPU processor operating at 2.67 GHz, featuring eight available CPUs and 8 GB of RAM. Finally, the output results by the FEA software contain warping deformation values. **Figure 5** shows the warping results of run 7 in the L9 array.

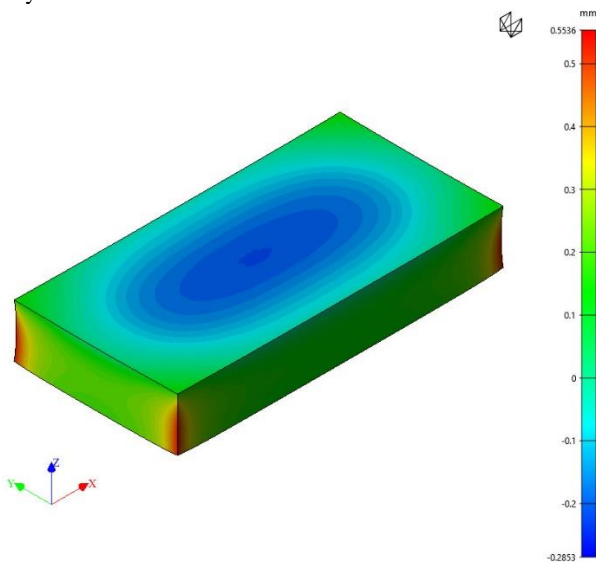


Figure 5. Warping results of Digimat-AM simulation for run 7

3. Results analysis and discussion

3.1. Probability plots

Table 2 presents the implementation of the Taguchi L9 orthogonal array (OA) along with the corresponding outcomes obtained from the numerical tests. The distribution of warping deformation results is quantified through probability plots to verify the normality assumption [52]. In this study, the Anderson-Darling (AD) test, a statistical technique widely employed for identifying outliers within a normal distribution, was employed [53]. The findings depicted in **Figure 6** reveal that the warping deformation results for all responses align closely with the fitted line. Furthermore, the Anderson-Darling (AD) statistics values exhibit comparably low values, and the p-value associated with the test surpasses the threshold of 0.05. These observations indicate that the data conform to a normal distribution. Consequently, the data is deemed suitable for further analysis and optimization, allowing for exploring additional insights.

Table 2. Taguchi L9 OA and the warping deformation results

| Run | BT [°C] | PS [mm/s] | CT [°C] | PT [°C] | Warping deformation [mm] |
|-----|------------|--------------|------------|------------|-----------------------------|
| 1 | 87 | 30 | 37 | 225 | 0.5549 |
| 2 | 87 | 45 | 40 | 230 | 0.5424 |
| 3 | 87 | 60 | 43 | 235 | 0.5304 |
| 4 | 90 | 30 | 40 | 235 | 0.5432 |
| 5 | 90 | 45 | 43 | 225 | 0.5533 |
| 6 | 90 | 60 | 37 | 230 | 0.5774 |
| 7 | 93 | 30 | 43 | 230 | 0.5536 |
| 8 | 93 | 45 | 37 | 235 | 0.5781 |
| 9 | 93 | 60 | 40 | 225 | 0.5884 |

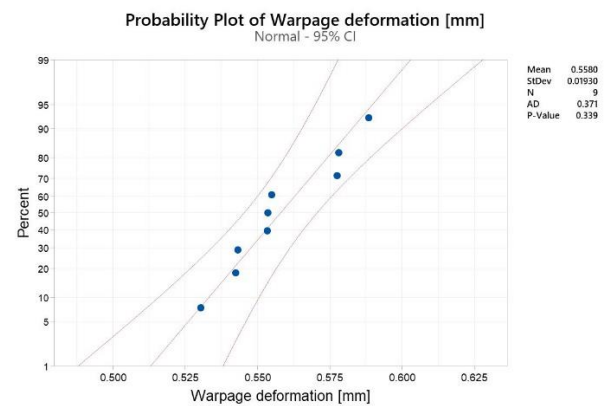


Figure 6. Probability plot of warping deformation response

3.2. MEP and Analysis of Variance of means for individual responses

Figure 7 and **Figure 8** provide a visual representation of the MEP analysis and the S/N ratio graph, respectively. An analysis of variance (ANOVA) was conducted at a 95% confidence level to assess the printing factors' main effects on individual responses. **Table 3** presents the ANOVA results for warping deformation, and the contribution percentages of each parameter in minimizing warping deformation were determined. Based on the computed p-values, it is evident that all the considered factors in this study exhibited statistical significance. These p-values serve as essential indicators of the strength of the associations between the factors and the observed variations in warping deformation. In this context, the obtained p-values were found to be below the predetermined threshold of 0.05, signifying a 95% confidence level. Among the investigated factors, bed temperature emerged as the most significant factor, contributing 47.75% towards minimizing warping deformation. Following closely was the chamber temperature, contributing 29.9%. The printing temperature and speed contributed 11.27% and 11.07%, respectively. The outcomes of this study are consistent with the prior research conducted by Stephens et al. [36]. In their study, the authors examined warping deformation in ABS samples produced using a cost-effective FDM printer equipped with a closed chamber to control the chamber temperature. Similar to the present investigation, they considered printing temperature, bed temperature, printing speed, and chamber temperature as the factors of interest. The results from Stephens et al.'s research revealed that the bed temperature exhibited the highest significance, contributing approximately 54.48% to

reducing warping deformation. Following closely, the chamber temperature demonstrated a contribution of approximately 39.87%. These findings align with and corroborate the observations made in the current study, serving as a valuable validation of the accuracy and reliability of this numerical model in predicting the influential factors for minimizing warping deformation in ABS-MEX printing.

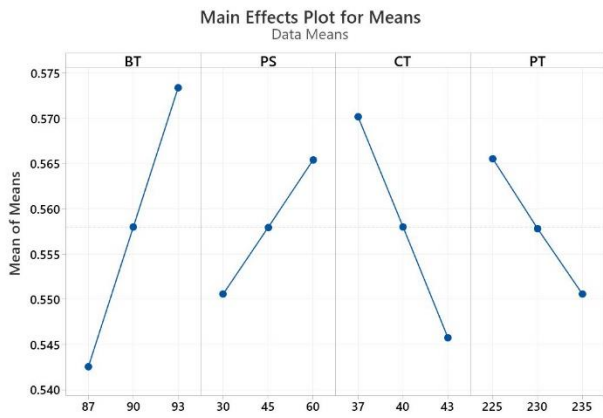


Figure 7. Mean effects plot for warping deformation

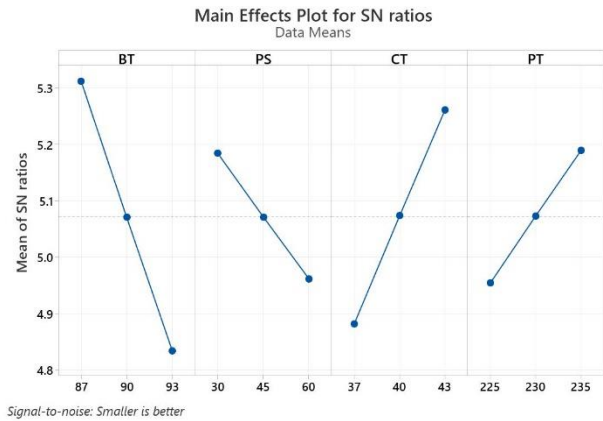


Figure 8. S/N ratio plot for warping deformation

Table 3. ANOVA for individual responses

| Source | DF | Seq SS | Contribution | Adj SS | Adj MS | F-Value | P-Value |
|--------|----|----------|--------------|----------|----------|----------|---------|
| BT | 2 | 0.001423 | 47.75% | 0.001423 | 0.001423 | 42161.78 | 0.00 |
| PS | 2 | 0.000330 | 11.08% | 0.000330 | 0.000330 | 9779.01 | 0.00 |
| CT | 2 | 0.000891 | 29.89% | 0.000891 | 0.000891 | 26388.20 | 0.00 |
| PT | 2 | 0.000336 | 11.28% | 0.000336 | 0.000336 | 9955.60 | 0.00 |
| Error | 0 | 0.00 | 0.00% | 0.00 | 0.00 | | |
| Total | 8 | 0.002980 | 100.00% | | | | |

3.3. Confirmation test

As depicted in Figure 8, the optimization of printing factors led to the minimization of warping deformation. Specifically, selecting a bed temperature of 87°C (first level), a printing speed of 30 mm/s (first level), a chamber temperature of 43°C (third level), and a printing temperature of 235°C (third level) resulted in the reduced warping deformation, as indicated by the graph. A confirmation simulation was conducted to validate and ensure the reliability of the abovementioned optimum level of printing factors determined through the Taguchi technique. This simulation aimed to assess and

confirm the quality response regarding warping deformation. The warping deformation observed in the confirmation simulation was measured at 0.5175 mm, which was less than the lowest value obtained in the previous results. This outcome indicates that the chosen optimal values of printing factors effectively minimized warping deformation. Hence, it can be concluded that the Taguchi technique successfully facilitated the determination of an optimal set of printing factors, demonstrating its efficiency in optimizing the printing process and improving the quality of the final printed parts.

4. Conclusion

In this study, the authors aimed to evaluate the thermal related factors of the material extrusion process, specifically focusing on warping deformation in ABS samples. The factors investigated included bed temperature, printing speed, chamber temperature, and printing temperature. To overcome the challenges associated with cost and time constraints in laboratory studies, a simulation approach employing numerical techniques and the Digimat-AM software's finite element model was utilized to investigate warping deformation. The Taguchi technique was utilized, involving 9 runs according to the number of process factors and their respective levels, to perform the necessary data for statistical analysis. This research contributes to understanding the thermal evaluation of material extrusion process factors and their influence on warping deformation in ABS samples. The utilization of numerical simulation and the Taguchi method allows for systematic analysis and optimization of the printing factors, leading to improved dimensional accuracy and reduced warping deformation. These findings provide valuable insights for the optimization of material extrusion processes and enhance the understanding of the interactions between process factors and warping deformation in material extrusion additive manufacturing.

Acknowledgments

No Acknowledgements

References

- [1] A. Dasgupta and P. Dutta, "A Comprehensive Review on 3D Printing Technology: Current Applications and Challenges," *Jordan Journal of Mechanical and Industrial Engineering*, vol. 16, no. 4, pp. 529–542, 2022.
- [2] T. S. Tshephe, S. O. Akinwamide, E. Olevsky, and P. A. Olubambi, "Additive manufacturing of titanium-based alloys- A review of methods, properties, challenges, and prospects," *Heliyon*, vol. 8, no. 3, p. e09041, Mar. 2022, doi: 10.1016/j.heliyon.2022.e09041.
- [3] H. Alzyod and P. Ficzero, "POTENTIAL APPLICATIONS OF ADDITIVE MANUFACTURING TECHNOLOGIES IN THE VEHICLE INDUSTRY," *Design of Machines and Structures*, vol. 11, no. 2, pp. 5–13, 2021.
- [4] R. Winarso, P. W. Anggoro, R. Ismail, J. Jamari, and A. P. Bayuseno, "Application of fused deposition modeling (FDM) on bone scaffold manufacturing process: A review," *Heliyon*, vol. 8, no. 11, p. e11701, Nov. 2022, doi: 10.1016/j.heliyon.2022.e11701.
- [5] Á. M. Horváth and P. Ficzero, "Rapid prototyping in medical sciences," *Production Engineering Archives*, vol. 8, pp. 28–31, Sep. 2015, doi: 10.30657/pea.2015.08.07.
- [6] A. Le-Bail, B. C. Maniglia, and P. Le-Bail, "Recent advances and future perspective in additive manufacturing of foods based on 3D printing," *Curr Opin Food Sci*, vol. 35, pp. 54–64, Oct. 2020, doi: 10.1016/j.cofs.2020.01.009.

- [7] T. Alsardia, L. Lovas, and P. Ficzer, "Prototype for fit investigation," *Design of Machines and Structures*, vol. 11, no. 1, pp. 5–15, 2021, doi: 10.32972/dms.2021.001.
- [8] H. Alzyod, J. Takacs, and P. Ficzer, "Improving surface smoothness in FDM parts through ironing post-processing," *Journal of Reinforced Plastics and Composites*, p. 073168442311730, Apr. 2023, doi: 10.1177/07316844231173059.
- [9] J. M. Jafferson and D. Chatterjee, "A review on polymeric materials in additive manufacturing," *Mater Today Proc.*, vol. 46, pp. 1349–1365, 2021, doi: 10.1016/j.matpr.2021.02.485.
- [10] Y. Tlegenov, G. S. Hong, and W. F. Lu, "Nozzle condition monitoring in 3D printing," *Robot Comput Integr Manuf.*, vol. 54, pp. 45–55, Dec. 2018, doi: 10.1016/j.rcim.2018.05.010.
- [11] H. Alzyod and P. Ficzer, "Material-Dependent Effect of Common Printing Parameters on Residual Stress and Warpage Deformation in 3D Printing: A Comprehensive Finite Element Analysis Study," *Polymers (Basel)*, vol. 15, no. 13, p. 2893, Jun. 2023, doi: 10.3390/polym15132893.
- [12] A. Hadny, Q. Ayun, J. Triyono, and E. Pujiyanto, "Optimization of Injection Molding Simulation of Bioabsorbable Bone Screw Using Taguchi Method and Particle Swarm Optimization," *Jordan Journal of Mechanical and Industrial Engineering*, vol. 16, no. 2, pp. 319–325, 2022.
- [13] S. G. Ghalme, "Improving Mechanical Properties of Rice Husk and Straw Fiber Reinforced Polymer Composite through Reinforcement Optimization," *Jordan Journal of Mechanical and Industrial Engineering*, vol. 15, no. 5, pp. 411–417, 2021.
- [14] R. Balcha, P. J. Ramulu, and B. B. Tesfamariam, "Mechanical Behaviour Assessment of Banana Fibres Reinforced Polymeric Composite with Aluminium-Powder Filler.," *Jordan Journal of Mechanical and Industrial Engineering*, vol. 17, no. 2, 2023.
- [15] A. A. Rahman, O. J. Adeboye, A. Adebayo, and M. R. Salleh, "Behaviour and Some Properties of Wood Plastic Composite Made from Recycled Polypropylene and Rubberwood," *Jordan Journal of Mechanical and Industrial Engineering*, vol. 17, no. 2, 2023.
- [16] H. Alzyod and P. Ficzer, "The Influence of the Layer Orientation on Ultimate Tensile Strength of 3D Printed Poly-lactic Acid," *Jordan Journal of Mechanical and Industrial Engineering*, vol. 16, no. 3, pp. 361–367, 2022.
- [17] H. Alzyod and P. Ficzer, "Optimizing fused filament fabrication process parameters for quality enhancement of PA12 parts using numerical modeling and taguchi method," *Heliyon*, vol. 9, no. 3, p. e14445, Mar. 2023, doi: 10.1016/j.heliyon.2023.e14445.
- [18] C. C. Ikeagwuani, D. C. Nwonu, C. K. Ugwu, and C. C. Agu, "Process parameters optimization for eco-friendly high strength sandcrete block using Taguchi method," *Heliyon*, vol. 6, no. 6, p. e04276, Jun. 2020, doi: 10.1016/j.heliyon.2020.e04276.
- [19] C. Tosto, J. Tirillò, F. Sarasini, C. Sergi, and G. Cicala, "Fused Deposition Modeling Parameter Optimization for Cost-Effective Metal Part Printing," *Polymers (Basel)*, vol. 14, no. 16, p. 3264, Aug. 2022, doi: 10.3390/polym14163264.
- [20] R. Paz, R. Moriche, M. Monzón, and J. García, "Influence of Manufacturing Parameters and Post Processing on the Electrical Conductivity of Extrusion-Based 3D Printed Nanocomposite Parts," *Polymers (Basel)*, vol. 12, no. 4, p. 733, Mar. 2020, doi: 10.3390/polym12040733.
- [21] I. Buj-Corral, A. Bagheri, and M. Sivatte-Adroer, "Effect of Printing Parameters on Dimensional Error, Surface Roughness and Porosity of FFF Printed Parts with Grid Structure," *Polymers (Basel)*, vol. 13, no. 8, p. 1213, Apr. 2021, doi: 10.3390/polym13081213.
- [22] A. D. Tura and H. B. Mamo, "Characterization and parametric optimization of additive manufacturing process for enhancing mechanical properties," *Heliyon*, vol. 8, no. 7, p. e09832, Jul. 2022, doi: 10.1016/j.heliyon.2022.e09832.
- [23] A. Z. Hameed, S. Aravind Raj, J. Kandasamy, M. A. Shahzad, and M. A. Baghdadi, "3D Printing Parameter Optimization Using Taguchi Approach to Examine Acrylonitrile Styrene Acrylate (ASA) Mechanical Properties," *Polymers (Basel)*, vol. 14, no. 16, p. 3256, Aug. 2022, doi: 10.3390/polym14163256.
- [24] I. Beşliu-Băncescu, I. Tamaşag, and L. Slătineanu, "Influence of 3D Printing Conditions on Some Physical-Mechanical and Technological Properties of PCL Wood-Based Polymer Parts Manufactured by FDM," *Polymers (Basel)*, vol. 15, no. 10, p. 2305, May 2023, doi: 10.3390/polym15102305.
- [25] H. Zhen, B. Zhao, L. Quan, and J. Fu, "Effect of 3D Printing Process Parameters and Heat Treatment Conditions on the Mechanical Properties and Microstructure of PEEK Parts," *Polymers (Basel)*, vol. 15, no. 9, p. 2209, May 2023, doi: 10.3390/polym15092209.
- [26] A. A. Rosli, R. K. Shuib, K. M. K. Ishak, Z. A. A. Hamid, M. K. Abdullah, and A. Rusli, "Influence of bed temperature on warpage, shrinkage and density of various acrylonitrile butadiene styrene (ABS) parts from fused deposition modelling (FDM)," 2020, p. 020072, doi: 10.1063/5.0015799.
- [27] J. S. Chohan, N. Mittal, and R. Kumar, "Parametric optimization of fused deposition modeling using learning enthusiasm enabled teaching learning based algorithm," *SN Appl Sci*, vol. 2, no. 12, p. 1978, Dec. 2020, doi: 10.1007/s42452-020-03818-4.
- [28] S. L. Messimer, A. E. Patterson, N. Muna, A. P. Deshpande, and T. Rocha Pereira, "Characterization and Processing Behavior of Heated Aluminum-Polycarbonate Composite Build Plates for the FDM Additive Manufacturing Process," *Journal of Manufacturing and Materials Processing*, vol. 2, no. 1, p. 12, Feb. 2018, doi: 10.3390/jmmp2010012.
- [29] D. Chaidas and J. D. Kechagias, "An investigation of PLA/W parts quality fabricated by FFF," *Materials and Manufacturing Processes*, vol. 37, no. 5, pp. 582–590, Apr. 2022, doi: 10.1080/10426914.2021.1944193.
- [30] S. Vyavahare, S. Kumar, and D. Panghal, "Experimental study of surface roughness, dimensional accuracy and time of fabrication of parts produced by fused deposition modelling," *Rapid Prototyp J*, vol. 26, no. 9, pp. 1535–1554, Jul. 2020, doi: 10.1108/RPJ-12-2019-0315.
- [31] M. Lee, Y.-S. Kwon, and C.-K. Lee, "Effect of warpage on the operation of a rapid cooling and heating device," *Journal of the Brazilian Society of Mechanical Sciences and Engineering*, vol. 41, no. 8, p. 322, Aug. 2019, doi: 10.1007/s40430-019-1806-8.
- [32] H. R. Vanaei *et al.*, "Toward the understanding of temperature effect on bonding strength, dimensions and geometry of 3D-printed parts," *J Mater Sci*, vol. 55, no. 29, pp. 14677–14689, Oct. 2020, doi: 10.1007/S10853-020-05057-9/FIGURES/12.
- [33] Y. Zhou, T. Nyberg, G. Xiong, and D. Liu, "Temperature Analysis in the Fused Deposition Modeling Process," in *2016 3rd International Conference on Information Science and Control Engineering (ICISCE)*, Beijing, China: IEEE, Jul. 2016, pp. 678–682, doi: 10.1109/ICISCE.2016.150.
- [34] R. Kumrai-Woodruff and Q. Wang, "Temperature Control to Increase Inter-Layer Bonding Strength in Fused Deposition Modelling," in *Volume 6: 25th Design for Manufacturing and the Life Cycle Conference (DFMLC)*, American Society of Mechanical Engineers, Aug. 2020, doi: 10.1115/DETC2020-22342.
- [35] A. D'Amico and A. M. Peterson, "An adaptable FEA simulation of material extrusion additive manufacturing heat transfer in 3D," *Addit Manuf*, vol. 21, pp. 422–430, May 2018, doi: 10.1016/j.addma.2018.02.021.
- [36] C.-C. Kuo, Y.-R. Wu, M.-H. Li, and H.-W. Wu, "Minimizing warpage of ABS prototypes built with low-cost fused deposition modeling machine using developed closed-chamber and optimal process parameters," *The International Journal of Advanced Manufacturing Technology*, vol. 101, no. 1–4, pp. 593–602, Mar. 2019, doi: 10.1007/s00170-018-2969-7.
- [37] S. Sarkara, R. Mandala, N. Mondal, S. Chaudhuric, T. Mandald, and G. Majumdara, "Modelling and Prediction of Micro-hardness of Electroless Ni-P coatings Using Response Surface Methodology and Fuzzy Logic," *Jordan Journal of Mechanical and Industrial Engineering*, vol. 16, no. 5, 2022.
- [38] F. Sk and D. V. Kumar, "Optimization of Performance and Exhaust Emissions of a PFI SI Engine Operated with Iso-stoichiometric GEM Blends Using Response Surface

- Methodology,," *Jordan Journal of Mechanical and Industrial Engineering*, vol. 15, no. 2, 2021.
- [39] J. A. Taborda-Ríos, O. López-Botello, P. Zambrano-Robledo, L. A. Reyes-Osorío, and C. Garza, "Mechanical characterisation of a bamboo fibre/polylactic acid composite produced by fused deposition modelling," *Journal of Reinforced Plastics and Composites*, vol. 39, no. 23–24, pp. 932–944, Dec. 2020, doi: 10.1177/0731684420938434/ASSET/IMAGES/LARGE/10.1177_0731684420938434-FIG10.JPEG.
- [40] A. Sahoo, S. Tripathy, and D. K. Tripathy, "Parametric Optimization of Pulse TIG Welding Process during Joining of Dissimilar Tensile Steels Used in Automotive Industries,," *Jordan Journal of Mechanical and Industrial Engineering*, vol. 16, no. 5, 2022.
- [41] S. Palaniyappan, D. Veeman, N. kumar Sivakumar, and R. Shanmugam, "Optimization of compressive property for the development of triply periodic minimal surface lattice structure on polylactic acid polymeric material," *Journal of Reinforced Plastics and Composites*, May 2022, doi: 10.1177/07316844221099582/ASSET/IMAGES/LARGE/10.1177_07316844221099582-FIG14.JPEG.
- [42] D. Veeman, S. Palaniyappan, G. J. Surendhar, and R. Shanmugam, "Process optimization of compressive property and dimensional error on wood polylactic acid gyroid-structured polymer composite," *Journal of Reinforced Plastics and Composites*, May 2022, doi: 10.1177/07316844221096486/ASSET/IMAGES/LARGE/10.1177_07316844221096486-FIG11.JPEG.
- [43] S. T. Ly and J. Y. Kim, "4D printing – fused deposition modeling printing with thermal-responsive shape memory polymers," *International Journal of Precision Engineering and Manufacturing-Green Technology*, vol. 4, no. 3, pp. 267–272, Jul. 2017, doi: 10.1007/s40684-017-0032-z.
- [44] A. Antony Samy, A. Golbang, E. Harkin-Jones, E. Archer, and A. McIlhagger, "Prediction of part distortion in Fused Deposition Modelling (FDM) of semi-crystalline polymers via COMSOL: Effect of printing conditions," *CIRP J Manuf Sci Technol*, vol. 33, pp. 443–453, May 2021, doi: 10.1016/j.cirpj.2021.04.012.
- [45] B. Hu *et al.*, "Improved design of fused deposition modeling equipment for 3D printing of high-performance PEEK parts," *Mechanics of Materials*, vol. 137, p. 103139, Oct. 2019, doi: 10.1016/j.mechmat.2019.103139.
- [46] A. A. Samy, A. Golbang, E. Harkin-Jones, E. Archer, D. Tormey, and A. McIlhagger, "Finite element analysis of residual stress and warpage in a 3D printed semi-crystalline polymer: Effect of ambient temperature and nozzle speed," *J Manuf Process*, vol. 70, pp. 389–399, Oct. 2021, doi: 10.1016/j.jmapro.2021.08.054.
- [47] A. Heydari, M. Mesgarpour, and M. R. Gharib, "Experimental and Numerical Study of Heat Transfer and Tensile Strength of Engineered Porous Fins to Estimate the Best Porosity,," *Jordan Journal of Mechanical and Industrial Engineering*, vol. 14, no. 3, 2020.
- [48] A. A. Lakhdari, I. I. Ovchinnikov, A. Seddak, and I. G. Ovchinnikov, "Numerical Modeling of Hydrogen Embrittlement of a Hollow Cylinder,," *Jordan Journal of Mechanical and Industrial Engineering*, vol. 12, no. 1, 2018.
- [49] H. F. AL-Qrimli, A. M. Abdelrhman, and K. S. Khiled, "Numerical and Theoretical Analysis of a Straight Bevel Gear Made from Orthotropic Materials,," *Jordan Journal of Mechanical and Industrial Engineering*, vol. 11, no. 1, 2017.
- [50] M. R. Talagani *et al.*, "Numerical simulation of big area additive manufacturing (3D printing) of a full size car," *SAMPE journal*, vol. 51, no. 4, pp. 27–36, 2015, Accessed: Oct. 21, 2021. [Online]. Available: www.mgc-a.com
- [51] P. Ficzer, L. Borbas, and A. Torok, "Validation of numerically simulated rapid-prototype model by photoelastic coating," *Acta Mechanica Slovaca*, vol. 18, no. 1, pp. 14–24, 2014, doi: 10.1515/mopa-2014-0002.
- [52] F. Zeqiri and B. Fejzaj, "Experimental Research and Mathematical Modeling of Parameters Affecting Cutting Tool Wear in Turning Process of Inconel 625," *Jordan Journal of Mechanical and Industrial Engineering*, vol. 16, no. 5, pp. 787–792, 2022.
- [53] M. A. Stephens, "EDF Statistics for Goodness of Fit and Some Comparisons," *J Am Stat Assoc*, vol. 69, no. 347, pp. 730–737, Sep. 1974, doi: 10.1080/01621459.1974.10480196.